



A02-13718

AIAA 2002-0287

**TLS: A New Two Level Simulation
Methodology for High-Reynolds LES**

K. Kemenov, S. Menon,
*School of Aerospace Engineering
Georgia Institute of Technology
Atlanta, Georgia 30332*

**40th AIAA Aerospace Sciences Meeting and
Exhibit**

January 14-17, 2002/ Reno, NV

TLS: A New Two Level Simulation Methodology for High-Reynolds LES

K. Kemenov*, S. Menon†
School of Aerospace Engineering
Georgia Institute of Technology
Atlanta, Georgia 30332

A new two-level simulation (TLS) approach, which treats resolved and small scales separately, is proposed and evaluated for applicability to 1D randomly forced Burgers turbulence and 3D high Reynolds number turbulent channel flow. The resolved and small-scale equations are derived based on the decomposition of the velocity into two components, and the large and small scales interact nonlinearly through interaction terms that are responsible for energy transfer between scales. In contrast to conventional LES approaches (where the small-scale field is approximated on the resolved grid using resolved properties), the small-scale evolution equations are solved directly on three orthogonal 1D grids (that are independent of the resolved 3D grid) to reconstruct the small-scale velocity field. The contribution of this small-scale field then appears as an effective forcing term in the resolved-scale equations. This TLS concept is first demonstrated using 1D randomly forced Burgers turbulence and then applied to study 3D turbulent channel flow.

1 Introduction

Simulation of very high Reynolds (Re) number wall-bounded flows is computationally very expensive because the near wall region has to be properly resolved in order to achieve accurate prediction. Past affordable studies using direct numerical simulations (DNS) have been limited to relatively low Re (500-2000 based on wall units).¹ However, the typical Re associated with wall-bounded flows of practical interest can be an order (or more) of magnitude higher. DNS is obviously impossible for such flows even with the projected speedup of the next generation computers and large-eddy simulations (LES) may be the only viable approach to study these flows. However, current LES methodology based on solving the spatially filtered LES equations with a model for the effect of unresolved motion have been only partially successful since it appears that even for LES of wall-bounded flows, the near wall resolution has to be close to the resolution needed for DNS.² Many past and on-going studies^{3,4} are investigating approaches that will allow a reduction of the near wall resolution without sacrificing accuracy. Although some significant progress has been achieved in these studies, there still remain many unresolved issues. In particular, the ability to carry out accurate LES of high- Re wall-bounded flows that transition to separated shear flows (a situation that occurs in many practical devices) has not yet been demonstrated.

The present effort is focused on developing a new approach for LES of high Re flows that departs significantly from conventional methods used in LES. In con-

ventional LES, the spatially filtered LES equations are solved on a “resolved” grid with a subgrid model that represents the effect of the unresolved scales of motion on the resolved motion. Current state-of-the-art subgrid models specify the grid scale as the characteristic length scale and differ primarily in the specification of the velocity scale. The algebraic Smagorinsky’s model⁵ uses the resolved rate-of-strain and the grid scale to estimate the velocity scale whereas, the one-equation Schumann model⁶ solves the transport equation for the subgrid kinetic energy to predict the length scale. Dynamic variants of these models⁷ attempt to estimate the “constant(s)” in the model, locally in space and time as a part of the solution, thereby eliminating the need to a priori assigning any constants. In this approach, scale similarity between the grid scale and a ‘test’ scale (which is typically twice the size of the grid scale) is employed to determine the coefficients of the model. However, in complex flows with no homogeneous directions, and in computational methodology that employs an unstructured grid topology, a truly localized (in space) scale-similar test filtering approach may not be stable or even definable. In the present effort, a new approach is being developed that is not constrained by these issues. This approach is described in some detail in the present paper.

The currently popular eddy viscosity SGS models have other problems as well since these models treat subgrid stresses as purely dissipative in nature and thus, fails to take into account important physical phenomena such as the inverse cascade of energy or backscatter - wherein energy is transferred from the smallest to the largest scale.^{8,9} Although models that employ an additional forcing term in the governing

*Graduate Research Assistant

†Professor, AIAA Associate Fellow

Copyright © 2002 by Menon, Kemenov. Published by the American Institute of Aeronautics and Astronautics, Inc. with permission.

equation¹⁰⁻¹² have been proposed to model backscatter, these models still remain un-validated for high Reynolds number turbulent flows. The simulation approach demonstrated in this paper obviates the need to define a subgrid eddy viscosity and allows full two-way energy transfer to be incorporated within a single formulation. Thus, in the proposed TLS formulation, both forward and back scatter effects are included without any a priori model specification.

The present approach is similar to several alternative approaches (referred loosely here as “decomposition” approaches) that have emerged in literature recently. In contrast to LES, where decomposition of turbulent velocity into two components, resolved and small-scale (unresolved), is introduced through spatial filtering and the major effort is concentrated on SGS modelling, in “decomposition” approaches considerable attention is devoted to modeling of small-scale velocity itself. This usually involves a derivation of governing equation for small-scale velocity with its subsequent simplification based on some physical arguments.

Clearly, a particular form of the small-scale equation as well as the precise meaning of the small-scale velocity depends on how the velocity field is decomposed into resolved and small-scale components. In recent studies,^{13,14} a two-fluid model has been proposed for two-dimensional turbulent flows. In this approach, small-scale equations are derived by simple subtraction of the filtered LES equation from the full Navier-Stokes equation. Then, by neglecting or modeling the interaction small scale terms leads to a linear form of the small-scale equation which somewhat resembles the RDT (rapid distortion theory) equation for turbulent velocity. The approach was further applied to study intermittency in decaying three-dimensional turbulence and renamed as the RDT model.¹⁵

An alternative approach in context of two-dimensional flows is the decomposition approach that employs a projection onto the eigenfunctions of the Stokes operator^{16,17} using a rigorous concept of approximate inertial manifolds (AIM). In physical sense, an AIM can be interpreted as a functional dependence of the small-scales upon resolved scales. A class of numerical schemes related to AIM and referred to as multilevel methods, have been proposed and applied to the study of two and three-dimensional turbulent flows.¹⁸ In a similar vein, a variational multi-scale method^{19,20} has been used to study decaying isotropic turbulence in spectral space.²¹ However, in this approach, the resolved and small-scale equations are obtained as a projection, respectively on the first half and the second half of the (Fourier) resolvable modes with a subsequent correction of the small-scale equations by adding an eddy viscosity type term to account of the subgrid scale effects on the second half of the resolvable scales (which are considered to represent small

scales in the multi-scale formulation).

Yet another somewhat related approach explicitly models the small-scale velocity field using a subgrid-scale velocity estimation approach.¹² In this model, the small-scale equation is not considered, instead the unfiltered velocity is approximated by expanding the resolved velocity to a scale that is two times smaller than the grid scale. That is, the resolved or LES equations are solved on twice-finer grid and then the solution is interpreted as an approximation to the sum of resolved and small-scale velocities which makes it possible to estimate the small-scale velocity and the subgrid stresses explicitly. Other approaches that consider direct modeling of small-scale velocity field via heuristic stochastic models have also been proposed, such as the small-scale fractal interpolation procedure²² or the additive turbulent decomposition (ATD).²³

In this paper, a two-level simulation (TLS) methodology is discussed in which both the resolved and unresolved scales of motion are simulated within a single simulation model. Regardless of how this approach is implemented it is apparent that if both the resolved and unresolved scales are simulated in three dimensions then this approach is no different than a DNS, and therefore, unviable. In order to implement this approach within the context of LES, we have developed a new approach in which the resolved scale motion are simulated using a ‘large-scale’ model that is forced by the unresolved motion. The unresolved motion (i.e., the subgrid flow field) evolves on another grid that is locally one-dimensional. This reduction in dimensionality allows the coupled TLS approach to be computationally feasible and applicable to high Re flow simulations.

In this paper, the mathematical formulation of the TLS approach is first developed and used to simulate one-dimensional Burger’s turbulence. Then, the formulation is extended to simulate three-dimensional channel flows.

2 Formulation

We begin the TLS formulation by first describing the decomposition method as applied to the one-dimensional Burger’s equation and then extending it to the full three-dimensional Navier-Stokes equations.

2.1 Two-Scale decomposition of the Burgers equation

We consider the one dimensional Burgers equation with a large scale random forcing $f(x, t)$:

$$\frac{\partial u}{\partial t} + \frac{1}{2} \frac{\partial uu}{\partial x} = \nu \frac{\partial^2 u}{\partial x^2} + f(x, t), \quad (1)$$

subject to the boundary and initial conditions:

$$u(0, t) = a, \quad u(L, t) = b, \quad u(x, 0) = \varphi_0(x) \quad (2)$$

We split the velocity field into large-scale and small-scale components:

$$u(x, t) = u_r(x, t) + u_s(x, t), \quad (3)$$

where the resolved scale is defined as a filtered quantity with respect to some spatial filter $h_r(x)$,

$$u_r(x, t) = \int_{-\infty}^{+\infty} u(y, t) h_r(x - y) dy \quad (4)$$

Although spatial filtering is not explicitly required in the TLS formulation, for demonstration purposes, we consider both spectral and physical space explicit filtering. When h_r is a spectral cut-off filter, it is convenient to define the small-scale spectral cut-off filter h_s as a filter that preserves scales between cut-off wave number k_c and some characteristic dissipation cut-off wave number k_η (which represents the smallest important scale). Then, the small-scale velocity is given as

$$u_s(x, t) = \int_{-\infty}^{+\infty} u(y, t) h_s(x - y) dy \quad (5)$$

In spectral space, the corresponding resolved and small-scale components of spectral velocity can be written as follows:

$$\hat{u}_r(k, t) = \hat{u}(k, t) \hat{h}_r(k) = \begin{cases} \hat{u}(k, t), & |k| \leq k_c \\ 0, & |k| > k_c \end{cases} \quad (6)$$

$$\hat{u}_s(k, t) = \hat{u}(k, t) \hat{h}_s(k) = \begin{cases} 0, & |k| \leq k_c, |k| > k_\eta \\ \hat{u}(k, t), & |k| > k_c, |k| \leq k_\eta \end{cases} \quad (7)$$

where spectral velocity $\hat{u}(k, t)$ is the Fourier transform of $u(x, t)$:

$$\hat{u}(k, t) = \frac{1}{2\pi} \int_{-\infty}^{+\infty} u(x, t) \exp(-ix) dx,$$

and $\hat{h}_r(k)$ is a spectral cut-off filter, $\hat{h}_s(k)$ is a spectral small-scale cut-off filter.

Inserting the decomposed velocity (3) into (1) and taking a convolution with resolved and small-scale filters give a coupled system of resolved and small-scale equations:

$$\frac{\partial u_r}{\partial t} + \frac{1}{2} \left[\frac{\partial u_r u_r}{\partial x} \right]_r = \nu \frac{\partial^2 u_r}{\partial x^2} - I_r(x, t) - S_r(x, t) + f(x, t), \quad (8)$$

$$\frac{\partial u_s}{\partial t} + \frac{1}{2} \left[\frac{\partial u_s u_s}{\partial x} \right]_s = \nu \frac{\partial^2 u_s}{\partial x^2} - R_s(x, t) - I_s(x, t), \quad (9)$$

where coupling terms are given as a convolution integrals:

$$I_r(x, t) = \left[\frac{\partial u_r u_s}{\partial x} \right]_r = \frac{1}{\pi} \int_{-\infty}^{+\infty} h_r(x - y) \frac{\partial u_r u_s}{\partial y} dy, \quad (10)$$

$$S_r(x, t) = \frac{1}{2} \left[\frac{\partial u_s u_s}{\partial x} \right]_r = \frac{1}{2\pi} \int_{-\infty}^{+\infty} h_r(x - y) \frac{\partial u_s u_s}{\partial y} dy, \quad (11)$$

$$I_s(x, t) = \left[\frac{\partial u_r u_s}{\partial x} \right]_s = \frac{1}{\pi} \int_{-\infty}^{+\infty} h_s(x - y) \frac{\partial u_r u_s}{\partial y} dy, \quad (12)$$

$$R_s(x, t) = \frac{1}{2} \left[\frac{\partial u_r u_r}{\partial x} \right]_s = \frac{1}{2\pi} \int_{-\infty}^{+\infty} h_s(x - y) \frac{\partial u_r u_r}{\partial y} dy, \quad (13)$$

We note that each term in the resolved scale equation (8) has a spectral support equal to $[-k_c, k_c]$ and constitutes a resolved quantity. Similarly each term in the small-scale equation (9) has a spectral support $[-k_\eta, -k_c] \cup [k_c, k_\eta]$ and therefore, represents a small-scale quantity. It also can be seen that the TLS analog of the Leonard stress $R_s(x, t)$ appears in the small scale equation as a forcing term since a nonlinear product of resolved velocities $u_r u_r$ has a spectral support that is larger (by a factor of two) of $u_r(x, t)$. We write this symbolically as

$$\text{supp}[u_r] = [-k_c, k_c], \quad \text{supp} \left[\frac{\partial u_r u_r}{\partial x} \right] = [-2k_c, 2k_c] \quad (14)$$

However, the spectral cut-off filter has a disadvantage of being applicable only in periodic domains because of the finite spectral support of the resolved velocity. This results in an infinite support of the resolved velocity in physical space which can be satisfied only by invoking a periodic domain assumption. For practical application of this TLS approach, periodic physical space domain is not acceptable. For physical space application, the small-scale velocity still can be defined based on the decomposition formula (3) rather than on explicit convolution integral. Thus, in a general case we define the small-scale quantities as

$$\begin{aligned} u_s(x, t) &= u(x, t) - u_r(x, t) \\ I_s(x, t) &= I(x, t) - I_r(x, t) \\ R_s(x, t) &= R(x, t) - R_r(x, t) \\ S_s(x, t) &= S(x, t) - S_r(x, t) \end{aligned} \quad (15)$$

Subtracting the resolved scale equation (8) from the original Burgers equation and applying the above definition produces exactly the same form of the small-scale equation (9) (which was obtained using the spectral cut-off filter). Note that, the resolved scale equation (8) is in the form of the LES equation:

$$\frac{\partial u_r}{\partial t} + \frac{1}{2} \frac{\partial u_r u_r}{\partial x} = \nu \frac{\partial^2 u_r}{\partial x^2} + \frac{\partial \tau_{sgs}}{\partial x} + f(x, t), \quad (16)$$

However, here the ‘‘subgrid’’ stress term is given as:

$$\begin{aligned} \frac{\partial \tau_{sgs}}{\partial x} &= \frac{1}{2} \frac{\partial u_r u_r}{\partial x} - \frac{1}{2} \left[\frac{\partial u_r u_r}{\partial x} \right]_r - I_r(x, t) - S_r(x, t) \\ &= R_s(x, t) - I_r(x, t) - S_r(x, t). \end{aligned} \quad (17)$$

To assess the role of the interaction terms in energy transfer between scales it is convenient to analyze spectral energy equations for resolved and small scales. Multiplying the resolved and small-scale equations in spectral space by the complex conjugates of the resolved and small-scale velocities results in an equation for the resolved spectral energy \widehat{E}_r and for the small-scale spectral energy \widehat{E}_s :

$$\frac{\partial \widehat{E}_r}{\partial t} + \widehat{T}_r(k, t) + k^2 \nu \widehat{E}_r = \widehat{F}(k, t) + \widehat{E}_r^b(k, t) + \widehat{E}_r^f(k, t) \quad (18)$$

$$\frac{\partial \widehat{E}_s}{\partial t} + \widehat{T}_s(k, t) + k^2 \nu \widehat{E}_s = \widehat{E}_s^b(k, t) + \widehat{E}_s^f(k, t) \quad (19)$$

where the source terms represent energy spectra of the scale interaction term and are defined in spectral space as:

$$\widehat{E}_r^b = \frac{1}{2} \Re(\widehat{S}_r \widehat{u}_r^* + \widehat{S}_r^* \widehat{u}_r), \quad \widehat{E}_s^b = \frac{1}{2} \Re(\widehat{I}_s \widehat{u}_s^* + \widehat{I}_s^* \widehat{u}_s), \quad (20)$$

$$\widehat{E}_r^f = \frac{1}{2} \Re(\widehat{I}_r \widehat{u}_r^* + \widehat{I}_r^* \widehat{u}_r), \quad \widehat{E}_s^f = \frac{1}{2} \Re(\widehat{R}_s \widehat{u}_s^* + \widehat{R}_s^* \widehat{u}_s), \quad (21)$$

Here, \widehat{u}_r^* is the complex conjugate to \widehat{u}_r and \Re is the real part. The sign of each energy source term defines a direction in which energy is transferred due to an action of a corresponding interaction term. For example, the interaction term $\widehat{R}_s(x, t)$ would supply energy to small scales if $\widehat{E}_s^f(k, t)$ is positive. Similarly, the interaction term $\widehat{I}_r(x, t)$ would remove energy from large scales if $\widehat{E}_r^f(k, t)$ is negative.

In this paper, we study the role of these interaction terms in energy transfer between scales to determine how energy is transferred from the large to the small scales and vice versa.

2.2 Two-Scale decomposition of the 3D Navier-Stokes equations

The methodology described above is applicable to the 1D Burger's equation. However, for more practical applications, we need to do a similar decomposition in 3D flows. To demonstrate this approach for 3D flows, we consider the incompressible Navier-Stokes equations:

$$\frac{\partial u_i}{\partial t} + \frac{\partial u_i u_j}{\partial x_j} = -\frac{\partial p}{\partial x_i} + \nu \frac{\partial^2 u_i}{\partial x_j^2} \quad (22)$$

$$\frac{\partial u_i}{\partial x_i} = 0, \quad (23)$$

and split the velocity field into resolved and small-scale components as noted earlier

$$u_i(\bar{x}, t) = u_i^r(\bar{x}, t) + u_i^s(\bar{x}, t). \quad (24)$$

On applying this splitting to the Navier-Stokes equation produces the following resolved scale equations:

$$\frac{\partial u_i^r}{\partial t} + \left[\frac{\partial u_i^r u_j^r}{\partial x_j} \right]_r = -\frac{\partial p^r}{\partial x_i} + \nu \frac{\partial^2 u_i^r}{\partial x_j^2} - S_i^r(\bar{x}, t) - I_i^r(\bar{x}, t), \quad (25)$$

$$\frac{\partial u_i^r}{\partial x_i} = 0$$

where scale interaction terms on the right hand side are given as

$$I_i^r(\bar{x}, t) = \left[\frac{\partial}{\partial x_j} (u_i^r u_j^s + u_j^r u_i^s) \right]_r \quad (26)$$

$$S_i^r(\bar{x}, t) = \left[\frac{\partial u_i^s u_j^s}{\partial x_j} \right]_r$$

Here, $[\cdot]_r$ indicate terms that are resolved on the "large" scale grid.

The small-scale equations are obtained by subtracting the resolved equations from the original Navier-Stokes equations. This gives

$$\frac{\partial u_i^s}{\partial t} + \left[\frac{\partial u_i^s u_j^s}{\partial x_j} \right]_s = -\frac{\partial p^s}{\partial x_i} + \nu \frac{\partial^2 u_i^s}{\partial x_j^2} - R_i^s(\bar{x}, t) - I_i^s(\bar{x}, t) \quad (27)$$

$$\frac{\partial u_i^s}{\partial x_i} = 0$$

Here, all small-scale quantity are defined based on decomposition

$$R_i^s = \left[\frac{\partial u_i^r u_j^r}{\partial x_j} \right]_s \equiv R_i - R_i^r = \frac{\partial u_i^r u_j^r}{\partial x_j} - \left[\frac{\partial u_i^r u_j^r}{\partial x_j} \right]_r \quad (28)$$

$$S_i^s = \left[\frac{\partial u_i^s u_j^s}{\partial x_j} \right]_s \equiv S_i - S_i^r = \frac{\partial u_i^s u_j^s}{\partial x_j} - \left[\frac{\partial u_i^s u_j^s}{\partial x_j} \right]_r \quad (29)$$

$$I_i^s = \left[\frac{\partial}{\partial x_j} (u_i^r u_j^s + u_j^r u_i^s) \right]_s \equiv I_i - I_i^r = \frac{\partial}{\partial x_j} (u_i^r u_j^s + u_j^r u_i^s) - I_i^r \quad (30)$$

The resolved scales affects the small-scale dynamics through the interaction terms $R_i^s(\bar{x}, t)$ and $I_i^s(\bar{x}, t)$ which are responsible for supplying/removing energy from the small-scales. In our model, we speculate that the derivative of the term $R_i^s(\bar{x}, t)$ is a primary supplier of energy to the small-scales. The small-scale equation (27) can be rewritten in the form containing only resolved parts of interaction terms (similar to the one-dimensional case described earlier):

$$\frac{\partial u_i^s}{\partial t} + \frac{\partial}{\partial x_j} \left((u_i^r + u_i^s)(u_j^r + u_j^s) \right) = -\frac{\partial p^s}{\partial x_i} + \nu \frac{\partial^2 u_i^s}{\partial x_j^2} + R_i^r + I_i^r + S_i^r. \quad (31)$$

The small-scale pressure equation follows from the standard Poisson equation for total pressure

$$\frac{\partial^2 p^s}{\partial x_j^2} = -\frac{\partial^2 p^r}{\partial x_j^2} - \frac{\partial (u_i^s + u_i^r)}{\partial x_j} \frac{\partial (u_j^s + u_j^r)}{\partial x_i}. \quad (32)$$

and can be viewed as an alternative to the small-scale continuity equation. Therefore, if the resolved scale velocity and pressure fields are known, the small-scale velocity and pressure can be reconstructed by solving the above two equations.

A numerical simulation of the above small-scale equations is quite challenging and will require computational effort similar to that for a DNS. Therefore, to model the small-scale turbulent velocity field efficiently and with a high physical fidelity, the small-scale equations must be simplified while retaining the underlying picture of scale interaction. This is described in the next section.

3 Numerical Implementation

This section summarizes the numerical implementation of the TLS formulation in both the 1D Burger's and 3D N-S formulation.

3.1 Burger's Equation

The small-scale equation (9) is not in form suitable for computations since it contains the small scale component of the product of two small-scale velocities. It is more convenient to recast the equation in another (but equivalent) form by adding the resolved parts of corresponding product terms to both sides of the equation. After some rearrangements, this results in the following form of the small-scale equation

$$\frac{\partial u_s}{\partial t} + \frac{1}{2} \frac{\partial (u_s + u_r)^2}{\partial y} = \nu \frac{\partial^2 u_s}{\partial y^2} + R_r(y, t) + S_r(y, t) + I_r(y, t) \quad (33)$$

In the present numerical simulations we associate a coarse grid $\{x_i\}$ with the resolved scale coordinate x and a fine scale grid $\{y_j\}$ with the small-scale coordinate y . Thus, for a given resolved velocity $u_r(x)$ on the coarse grid we solve (33) on the fine grid. The resolved quantities $u_r(x)$ and $R_r(x)$ are known on the coarse grid and thus, can be interpolated on to the fine grid as piecewise linear functions. Note that, the interaction terms $S_r(y, t)$ and $I_r(y, t)$ are obtained automatically in the course of computation of the small-scale equation (33) and can be used to close the resolved equation (8). This suggests a following algorithm for the two-scale simulation of Burgers equation:

- At time t , having the known resolved velocity $u_r(x)$ on the coarse grid $\{x_i\}$, interpolate it on to the fine grid $\{y_j\}$ and compute the forcing term $R_r(y)$. Thus,

$$u_r(x) \longrightarrow u_r(y) \longrightarrow R_r(y) = \frac{1}{2} \left[\frac{\partial u_r u_r}{\partial y} \right]_r$$

- Solve (33) to find the small-scale velocity $u_s(y, t)$ on the fine grid $\{y_j\}$

- Compute the interaction terms $I_r(x)$, $S_r(x)$ on the coarse grid $\{x_i\}$

$$I_r(x) \longleftarrow I_r(y) = \left[\frac{\partial u_r u_s}{\partial y} \right]_r,$$

$$S_r(x) \longleftarrow S_r(y) = \frac{1}{2} \left[\frac{\partial u_s u_s}{\partial y} \right]_r;$$

- Advance the resolved velocity $u_r(x, t)$ at time $t + \Delta t_r$ by solving the resolved equation (8) on the coarse grid $\{x_i\}$.

The results of these simulations are discussed in this paper.

3.2 3D Channel Flow

As mentioned earlier, the full two scale simulation model is not viable due to DNS comparable resource requirement. In the light of this, we propose a new simplified model for reconstructing the small-scale velocity field. In some respect this is consistent with the framework of the One-Dimensional Turbulence (ODT) approach originally developed by Kerstein and co-workers^{24, 25}

In ODT approach, turbulent velocity and other properties are simulated along one-dimensional line of sight through a 3D turbulent flow. The reduction to 1D domain makes the model computationally efficient. However, a correct formulation and implementation of ODT model, as a closure for subgrid scale fluxes, is not straightforward and is still an area of active research.³ The baseline ODT model has a disadvantage since it is not able to take into account the effects of resolved velocity on the modeled small-scale velocity field, thus somewhat hindering a forward energy cascade picture. Here, we propose an extension of ODT to address this issue.

To model the small-scale turbulent velocity field in a 3D domain Ω , we consider a family of 1D ODT lines arranged as 3D lattice embedded in Ω . The family consists of three types of lines $\{l_1, l_2, l_3\}$ orthogonal each other and parallel to corresponding Cartesian coordinates x_i . The lines of each type intersects each other at a center of a cell which is defined by the resolved grid in the domain Ω . The line arrangement is shown in Fig.6. We model the 3D small-scale velocity field as a family of 1D small-scale velocity vector fields defined on the underlying family of lines $\{l_1, l_2, l_3\}$

$$u_i^s(\bar{x}, t) \longrightarrow u_{i,l_j}^s(l_j, t), \quad \bar{x} \in \Omega, \quad l_j \in R^1$$

The small-scale velocity field $u_{i,l_j}^s(l_j, t)$ can be viewed as a snapshot of the small-scale 3D turbulent field along the line $\{l_j\}$ somehow oriented in computational domain Ω (in principle, the orientation of this 1D line can be arbitrary but in the present effort is along the resolved grid lines). The small-scale velocity fields evolve according to simplified 1D governing

equations that can be obtained from the basic small-scale equation (31) by utilizing assumptions made in the definition of ODT model. Namely, since the velocities are defined on 1D lines, all derivatives with respect to directions other than along the line in consideration are set to zero. This gives a following system of ODT equations for small-scale velocities defined on the family of lines $\{l_1^{k_1}, l_2^{k_2}, l_3^{k_3}; k_j = 1, \dots, N_j; j = 1, 2, 3\}$, where N_j is the number of lines of j th type,

$$\frac{\partial u_{ij}^s}{\partial t} + \frac{\partial}{\partial l_j} \left((u_{ij}^r + u_{ij}^s)(u_{jj}^r + u_{jj}^s) \right) = \nu \frac{\partial^2 u_{ij}^s}{\partial l_j^2} + R_i^r + I_i^r + S_i^r \quad (34)$$

Here, the following notation is used: $u_{ij}^s(l_j, t) \equiv u_{i,l_j}^s(l_j, t)$ represents the i -th component of the small-scale velocity belonging to j -th type of line, the upper index corresponding to the line number in $l_j^{k_j}$ is also dropped for notation simplicity and interaction terms are defined on the j -th line, i.e., $R_i^r = R_i^r(l_j, t)$ and so on. The system of ODT equations (34) does not have pressure term because the continuity requirement for small-scale velocities defined on lines is relaxed.¹

For example, the ODT equations along l_1 lines (which are parallel to x -coordinate of the resolved grid) gives the following system of equations denoting for simplicity, $u_{i1}^s(l_1, t) \equiv (u^s, v^s, w^s)$:

$$\frac{\partial u^s}{\partial t} = \frac{\partial (u^s + u^r)^2}{\partial l_1} = \nu \frac{\partial^2 u^s}{\partial l_1^2} + \left[\frac{\partial (u^s + u^r)^2}{\partial l_1} \right]_r \quad (35)$$

$$\frac{\partial v^s}{\partial t} + \frac{\partial}{\partial l_1} \left((u^s + u^r)(v^s + v^r) \right) = \nu \frac{\partial^2 v^s}{\partial l_1^2} + \quad (36)$$

$$\left[\frac{\partial}{\partial l_1} \left((u^s + u^r)(v^s + v^r) \right) \right]_r$$

$$\frac{\partial w^s}{\partial t} + \frac{\partial}{\partial l_1} \left((u^s + u^r)(w^s + w^r) \right) = \nu \frac{\partial^2 w^s}{\partial l_1^2} + \quad (37)$$

$$\left[\frac{\partial}{\partial l_1} \left((u^s + u^r)(w^s + w^r) \right) \right]_r$$

The resolved velocity is assumed to be known on each line so the forcing terms on the right hand side can be easily computed. Note that, on different line the system will generate different small-scale fields since the resolved velocity is changing from line to line.

We apply our TLS approach to simulate 3D turbulent channel flow. The computational domain is parallelepiped $\Omega = 2\pi \times 2 \times \frac{2}{3}\pi$ which discretized by a coarse resolved grid with stretching in wall normal directions. The numerical algorithm, which is similar to the one used for the Burgers equation case, is

- At time t , having known resolved velocity $u_i^r(\bar{x}, t)$ on the coarse grid (obtained using a conventional

¹the straightforward enforcing of continuity equation on a line leads to trivial case of a constant velocity profile

staggered grid finite-volume scheme²⁶), interpolate it on each ODT line $\{l_j\}$ and compute the forcing term $R_i^r(l_j)$

$$u_i^r(\bar{x}) \rightarrow u_{ij}^r(l_j) \rightarrow R_i^r(l_j) = \left[\frac{\partial u_{ij}^r u_{ij}^r}{\partial l_j} \right]_r;$$

- Solve the ODT small-scale system (34) on each line with corresponding boundary condition to find $u_{ij}^s(l_j)$;
- Compute the interaction terms $I_i^r(\bar{x})$, $S_i^r(\bar{x})$ on the resolved (LES) grid

$$I_i^r(\bar{x}) \leftarrow I_i^r(l_j) = \left[\frac{\partial u_{ij}^r u_{ij}^s}{\partial l_j} \right]_r,$$

$$S_i^r(\bar{x}) \leftarrow S_i^r(l_j) = \left[\frac{\partial u_{ij}^s u_{ij}^s}{\partial l_j} \right]_r,$$

- Advance the resolved velocity $u_i^r(\bar{x}, t)$ at time $t + \Delta t_r$ by solving the resolved equation on the resolved grid.

3.3 Near-Wall ODT Implementation

Earlier, the ODT model was implemented primarily as a near wall model following the work done at Sandia.³ In this approach, the ODT domain was a 1D wall normal line in the *first* LES cell near the wall. This approach solves a reduced form on the 1D model described above in this first LES cell and the near-wall ODT was linked to a conventional LES model used in the rest of the domain. However, in this approach the velocity splitting into the small-scale (ODT) and the resolved (LES) velocities has a different meaning and constitutes a geometrical splitting rather than functional splitting adopted in TLS. As a result, the ODT velocity is defined only in the first boundary cell and evolves according to the following advection-diffusion equation:

$$\frac{\partial u_i^s}{\partial t} + \frac{\partial}{\partial x_j} (u_i^s V_j) = \nu \frac{\partial^2 u_i^s}{\partial x_j^2} - \frac{\partial}{\partial x_i} P^{LES} e_i, \quad (38)$$

where the vector $\bar{e} = (1, 0, 1)$ is introduced to neglect the pressure gradient in wall normal direction and V_j is the local advective velocity field defined as a time average of ODT velocity field over the LES time step. More details are given elsewhere.³

The ODT resolution in the first LES cell is fine enough to resolve the viscous sublayer and the buffer layer and therefore, the LES resolved grid did not have to resolve this region. As a result, significant reduction in computational effort is achieved by this method. However, this approach requires explicit coupling models to link the near-wall ODT with the conventional LES model away from the wall and special rules has to

be devised to allow the two disparate simulation procedures to be coupled together. Although very encouraging results were reported earlier³ and also achieved in the present study (see results discussed below), simulations also showed that the coupling of the two models is not very robust and in particular, the coupling algorithm had to be explicitly built around the actual numerical algorithm used for the LES model. Figure 13 shows schematically the coupling between the near-wall ODT with the LES model. More details are given elsewhere³ and therefore, not described here for brevity. The implication of this coupling is however, discussed in this paper.

It is worth noting here that the TLS model described in the previous section removes all the problems noted with the coupling of the near-wall ODT with LES and is applicable in any resolved scale numerical solver. Therefore, the final version of the TLS approach would involve a combination of the TLS model described in the previous section and the near-wall ODT. In this paper, we discuss the results of independent implementation of each of these model. The fully coupled model predictions will be reported in the near future.

4 Results and Discussion

4.1 Forced Burger's Turbulence

To study the role of the interaction terms we performed a series of numerical simulations of randomly forced Burgers equation on a periodic domain of length $L = 1$. For direct simulation (DNS) we used a fine resolution grid with $N_s = 16324$ grid points and viscosity coefficient equal to $\nu = 5 \cdot 10^{-6}$. Simulation was carried out for a time range $0 \leq t \leq 750$ using a second-order accurate predictor-corrector scheme. The forcing was simulated in physical space as a white random noise in x with zero mean. To mimic the TLS approach, the forcing was explicitly filtered in spectral space to suppress all modes beyond a force cut-off number k_f which was chosen to be approximately two time less than a scale separation cut-off number k_c , $\text{supp}(f(y, t)) = [-k_f, k_f]$. To separate scales into two components, a cut-off wave number was chosen in the inertial range and equal to $k_c = 128$.

The statistically steady turbulent solution was reached after approximately $t_{ss} = 50$. The time-averaged energy spectra of the interaction terms $\langle \hat{E}_r^f(k) \rangle_T$, $\langle \hat{E}_s^f(k) \rangle_T$, $\langle \hat{E}_r^b(k) \rangle_T$, $\langle \hat{E}_s^b(k) \rangle_T$ and the energy spectrum $\langle \hat{E}(k) \rangle_T$ are computed as an average of instantaneous spectra at times $t_j = t_{ss} + jT$, where t_{ss} is the time to establish the statistically steady state and $T = 10$.

To study the role the interaction term it is convenient to represent a coupled set of equations (8), (9) by a diagram as given in Fig.1.²

The upper part and the lower part of the diagram represent respectively, the resolved scale equation (8)

²all terms on the diagram are shown in spectral space

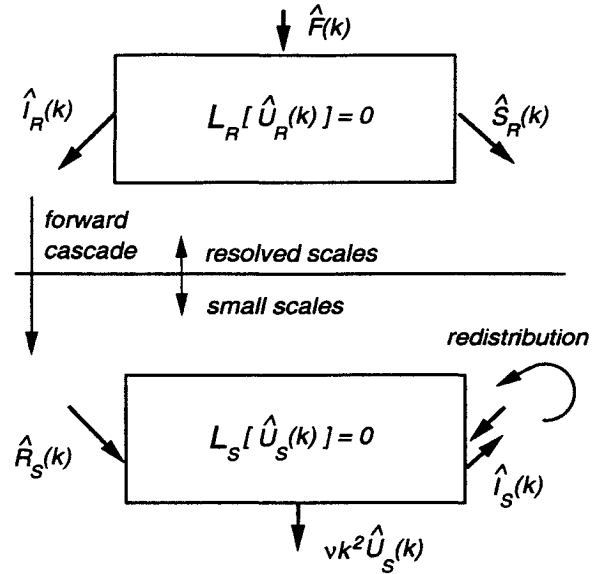


Fig. 1 Scale interaction diagram for Burgers turbulence; the upper part corresponds to LES.

and the small-scale equation (9). The effect of small scales on the resolved field enters through interaction terms $I_r(x, t)$ and $S_r(x, t)$. In conventional SGS models, the net effect of these terms is parametrized by the resolved velocity $u_r(x, t)$. Resolved scales, in their turn, also affect small-scale dynamics due to the terms $I_s(x, t)$ and $R_s(x, t)$. Equations shown in boxes are the right hand sides of equations (8), (9) and represent a non-viscous version of the Burgers equation restricted to resolved and small scales, respectively:

$$L_r[u_r] = \frac{\partial u_r}{\partial t} + \frac{1}{2} \left[\frac{\partial u_r u_r}{\partial x} \right]_r = 0,$$

$$L_s[u_s] = \frac{\partial u_s}{\partial t} + \frac{1}{2} \left[\frac{\partial u_s u_s}{\partial x} \right]_s = 0$$

Interaction terms are shown as arrows pointing at or out of a corresponding box in the scale diagram. We may associate the direction of interaction term arrows with a direction of energy transfer between scales. Based on the diagram it is easy to envision a qualitative scenario of scale interaction at the turbulent stationary state. An external random force $f(x, t)$ with a spectral support in low wave numbers pumps energy into the resolved scales. The role of the non-viscous operator $L_r[u_r]$ is to redistribute energy among resolved scales. Numerical simulations and statistical analysis of the resolved non-viscous Burgers equation, i.e., $L_r[u_r] = 0$, with smooth initial data was a subject of recent study²⁷ which revealed that solution exhibits a strong intrinsic chaotic dynamics with statistical equipartition of energy among all resolved modes.

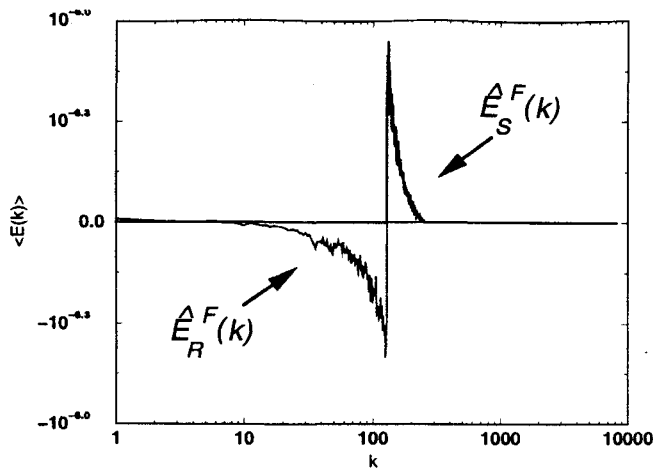


Fig. 2 Time averaged spectra $\langle \hat{E}_r^f(k) \rangle_T$, $\langle \hat{E}_s^f(k) \rangle_T$ of the interaction terms $\hat{I}_r(k)$, $\hat{R}_s(k)$.

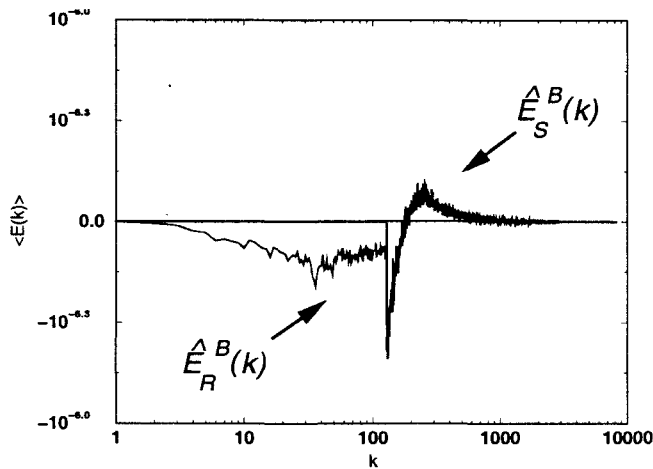


Fig. 3 Time averaged spectra $\langle \hat{E}_r^b(k) \rangle_T$, $\langle \hat{E}_s^b(k) \rangle_T$ of the interaction terms $\hat{S}_r(k)$, $\hat{I}_s(k)$.

The time-averaged energy spectra of the various interaction terms are shown in Figs. 2, 3. From Fig. 2 it is seen that the "resolved-small" interaction term $I_r(x, t)$ removes energy from large scales and therefore, acts as a sink of energy in the resolved scales. On the other hand, the interaction term $R_s(x, t)$ supplies energy to small scales and thus, plays a role of a source of energy. At the small scales, the energy is redistributed by a non-viscous nonlinear operator $L_s[u_s]$. Furthermore, a major portion of energy is also removed by viscous dissipation. The action of the other pair of interaction terms (on the right hand side of the diagram) is shown in Fig. 3. The resolved part of the "small-small" interaction term $S_r(x, t)$ removes energy from resolved scales and therefore acts as a sink of energy. The role of the "mixed" interaction term $I_s(x, t)$ is somewhat more complex. It removes energy from wave-numbers adjacent to the cut-off wave number k_c

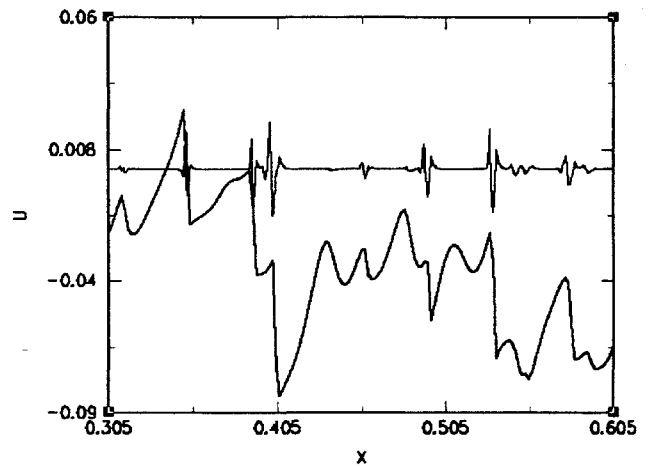
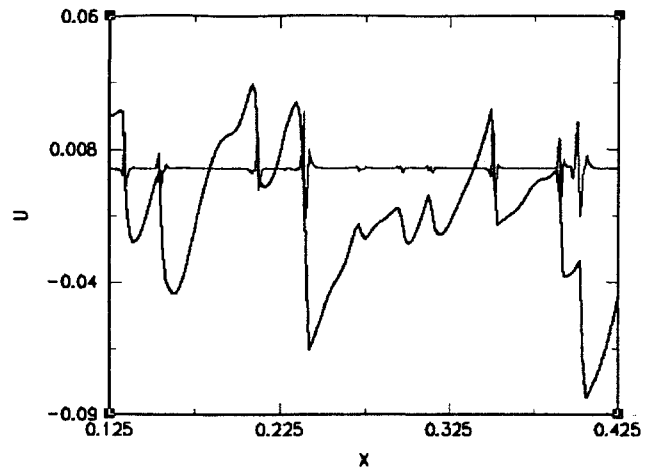


Fig. 4 Snapshots of the resolved and the small-scale velocities.

and supplies energy to higher wave numbers. This results in the overall redistribution energy effect in favor of the smaller scales. Thus, we may conclude that there is no backscatter of energy present in the case.

Note that, the overall picture of energy transfer and redistribution is independent of the choice of spatial filter. Time averaged spectra of the interaction terms for the case of physical box filter exhibit a similar behavior (and therefore, not shown here for brevity).

Typical instantaneous snapshots of the resolved and the small-scale velocity fields are shown in Figs. 4. One can see that the reconstructed small-scale velocity profile $u_s(y)$ captures a small-scale shock pattern relatively well. The "resolved-scale" interaction term $R_s(x)$ is the most important forcing term since it determines the topology of small-scale velocity field and thus, needs to be taken in account in simplified models for the the small-scales Eq(33). It is interesting to note that implicitly, this fact was used as a basis of

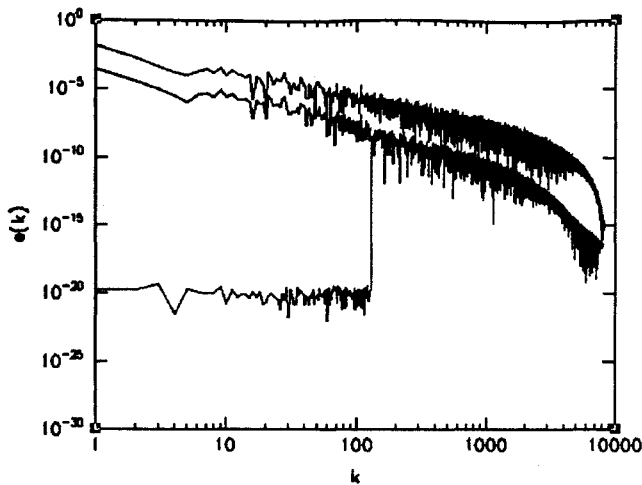


Fig. 5 Comparison of the resolved and small-scale spectra of TLS with DNS energy spectrum. Note that, the TLS spectra are shifted vertically to enable comparison. Clearly, the TLS approach captures the resolved spectra very accurately.

the subgrid estimation model.¹² Solving the Navier-Stokes equation on a grid which is two times finer than the original resolved grid gives an opportunity to capture a small-scale part of the nonlinear term, which is an analogue of $R_s(y)$ in our 1D dimensional case, and leads to more physically correct prediction of small-scale field.

Finally, to check the performance of our model we run the full TLS of Burgers equations using the coupled algorithm described earlier. The coupled system of the resolved scale equation (8) and the small-scale equation (33) are solved on a coarse grid $\{x_i, i = 1, \dots, N_r\}$ of size $N_r = 512$ and on a fine grid $\{y_j, j = 1, \dots, N_s\}$ of size $N_s = 16324$, respectively. Energy spectra of resolved velocity and small-scale velocity are compared with total energy spectrum $\hat{E}(k)$ (obtained using the full Burger's model as in a DNS) in Fig. 5. It is seen that in the region of resolved scales support a resolved velocity energy spectrum $\hat{E}_r(k)$ obtained with TLS approach is relatively well matched with the total DNS energy spectrum $\hat{E}(k)$. The small-scale spectra in the TLS approach is also reasonably resolved. Note that, unlike in classical LES where the resolved spectra typically begins to deviate (decay) from the DNS spectra as the cutoff wavenumber is approached, in the TLS approach, the resolved spectra show no such decay. This is one of the unique features of the TLS approach that is expected to play a major role in capturing high Re turbulent flows.

4.2 High-Re Channel Flows

3D TLS of high-Re channel flows have been conducted using a staggered grid technique.²⁶ A third-order low storage Runge-Kutta scheme was employed

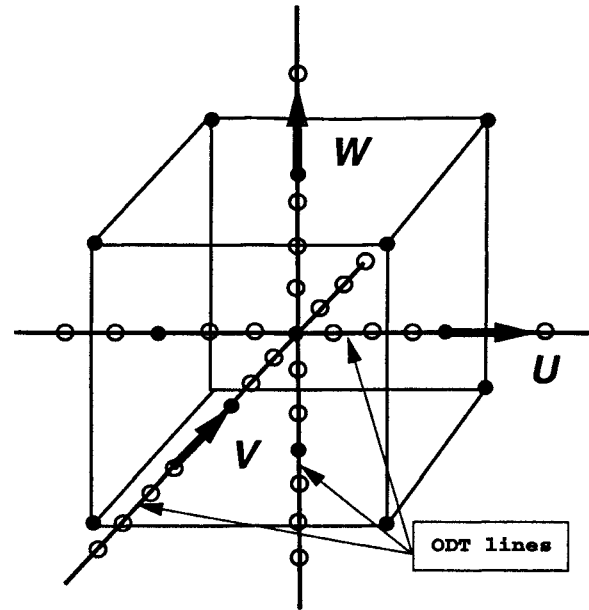


Fig. 6 The ODT line arrangement in TLS Model.

for temporal discretization.²⁸ This scheme is second-order accurate and employs the standard Germano's dynamics subgrid model for the baseline LES approach. For TLS application, the SGS model is removed and replaced by the terms described in the TLS formulation. The small-scale field is also simulated using the TLS 1D model described earlier. No special treatment of the near-wall cell (i.e., coupling with the near-wall ODT) is used in the present effort since the primary goal of this study is to evaluate the baseline TLS approach. Simulations for a $Re = 595$ (based on wall units) is performed in this initial effort since DNS data¹ is available for comparison. A resolution of $32 \times 32 \times 32$ is employed for the resolved field and the 1D ODT lines in the wall normal and periodic directions employed a resolution of 528 and 128 points respectively. Since the resolved domain is very coarse, the first grid point next to the wall is well outside the buffer layer (around $y^+ \approx 30$ and therefore, the near-wall turbulent field is not expected to be captured in the resolved field. However, the small-scale model is expected to capture some of this effect and therefore, resolved field profiles outside the wall region should evolve as if the near wall region is resolved. [As described in the following section, the near-wall profile can be captured quite accurately by the near-wall ODT model which we plan to integrate within the TLS formulation in the near future.]

The present simulation has not been carried out for sufficiently long time (due to some unanticipated delay in completing the computations) for detailed statistical analysis and furthermore, issues such as the resolved and small scale grid resolution effects have not yet been addressed. Therefore, the results reported be-

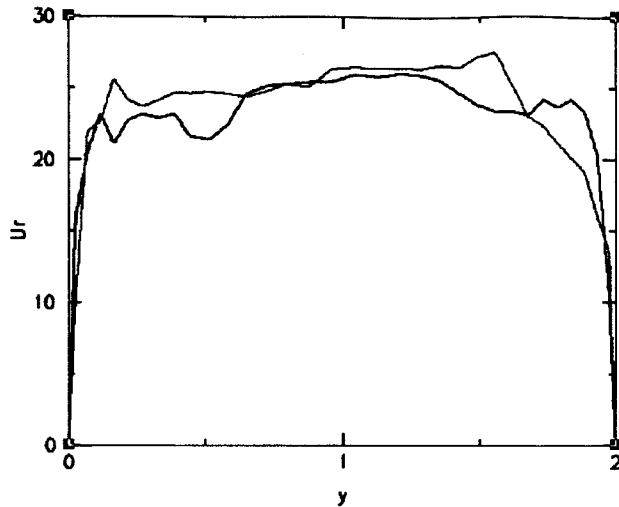


Fig. 7 The snapshot of the resolved streamwise velocity on two different wall-normal lines.

low (especially the higher moments) are not considered as the final converged solution. However, the preliminary results reported here demonstrate the potential of the TLS method. Note that, unlike classical LES SGS modeling, there are no adjustable “coefficient” or constants to manipulate in the present formulation.

Typical profiles of the streamwise small-scale and resolved velocities for two different wall normal lines are shown in Figs.7 and 8. It can be seen that fluctuations of the small-scale velocity is always of high intensity in the near wall region. Despite the fact that instantaneous small-scale profiles are not symmetric, a time averaged profile of the small-scale velocity exhibits clear symmetry, as shown in Fig.9. This shows that the small-scale model has been implemented in a consistent manner.

The mean profile of the total streamwise velocity $u^r(x_2) + u^s(x_2)$ along the wall-normal coordinate is shown in Fig.10. In general, the TLS profile is very similar to the DNS results especially in the near wall viscous sublayer region. However, away from the wall the TLS profile shows a higher resolved velocity magnitude. At present, reason for this not apparent, although the limited run time data that was used for this analysis could be a cause (the fact that the viscous sublayer is in good agreement suggests this as a possible explanation since the viscos region should converge faster than the log-layer). We will be addressing this issue in the immediate future.

The rms total velocity profiles are plotted in wall units in Fig.11. In spite of the fact that spanwise and wall-normal rms velocities are clearly underestimated, the more important streamwise velocity rms demonstrates the correct behavior in the near wall region. Again, the limited data that is used for the present

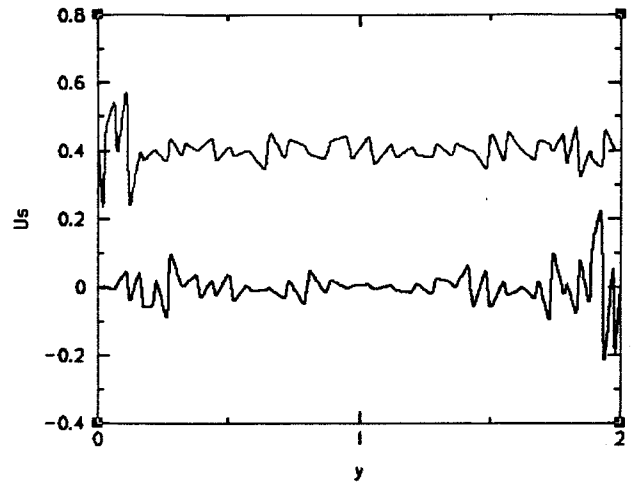


Fig. 8 The snapshot of the small-scale streamwise velocity on two different wall-normal lines. Note that one small-scale profile is shifted vertically from zero line for visualization.

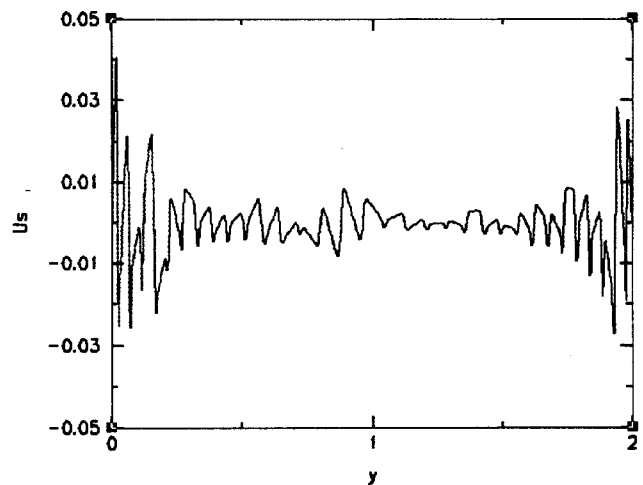


Fig. 9 The time averaged (over a small period of time) profile of the small-scale velocity on a one line from Fig.8.

statistical analysis may be the reason for the fluctuating behavior observed in these profiles.

Clearly, far away from the wall, the rms profiles should scale with outer coordinates, rather than y^+ . These plots are shown in Fig.12 with respect to non-dimensional wall normal direction y/δ . Again, the overall trends and relative magnitudes are consistent with what is expected in high Re channel flows.

4.3 Near-Wall ODT Issues

As mentioned earlier, simulations are also carried out in which the 1D ODT model was implemented only in first LES cell next to the wall and the standard

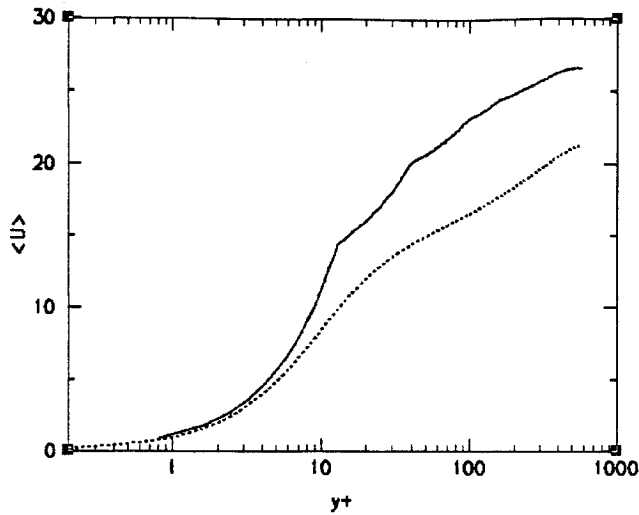


Fig. 10 The mean total streamwise velocity profile in wall units: solid line (TLS), dashed line (DNS).

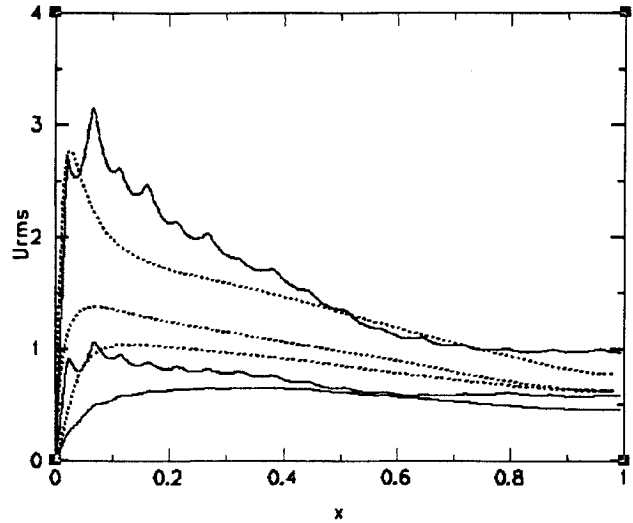


Fig. 12 Rms velocity profiles in wall units: solid line (TLS), dashed line (DNS).

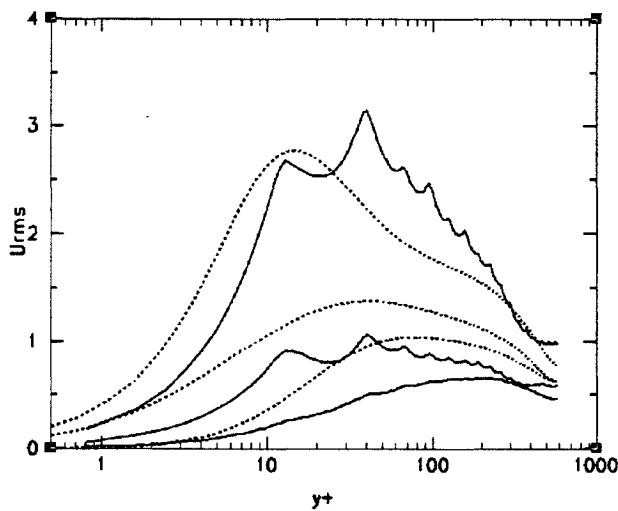


Fig. 11 Rms velocity profiles in wall units: solid line (TLS), dashed line (DNS).

LES model (using the Germano's dynamic model) is used in the rest of the domain. This approach essentially repeated the earlier study³ using the staggered grid solver described in the previous section. Since the results were similar, they are not repeated here. However, we briefly discuss some of the coupling issues (noted earlier) that we hope to eliminate using the TLS approach.

Figure 14 shows the turbulent fluctuation intensity in the wall normal direction using the original near-wall ODT formulation as described by Schmidt et al.³ and a version in which the coupling between the ODT and LES was modified in the LES overlap region (see

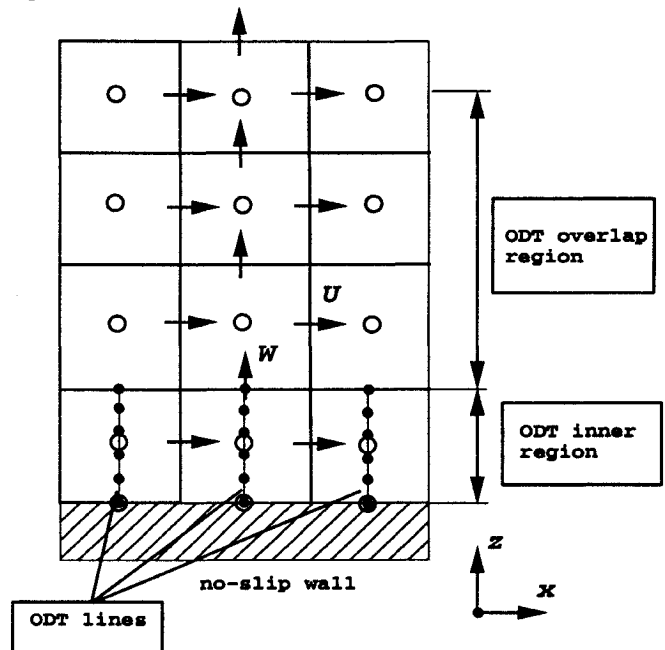


Fig. 13 The ODT line arrangement in the near-wall ODT Model.

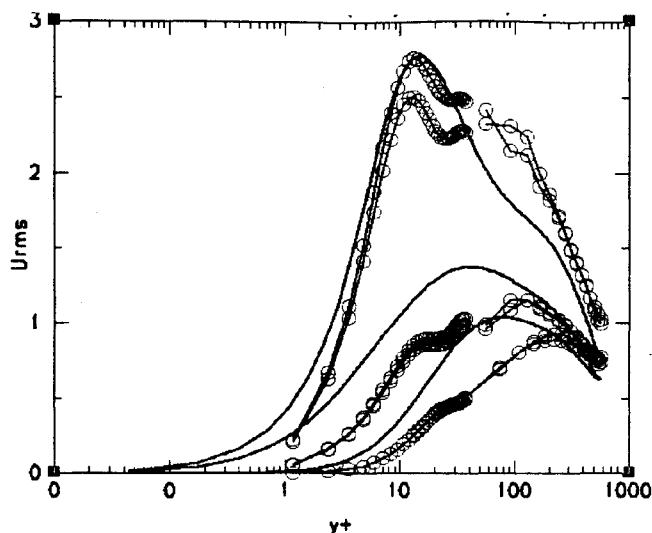


Fig. 14 Rms velocity profiles for two versions of near-wall ODT Model.

Fig. 13).

The DNS results are also shown for comparison. It can be seen that the near wall ODT can capture the viscous sublayer and the peak in the buffer layer reasonably well and that the modifications to the ODT-LES coupling can strongly effect the prediction near the overlap region.

It is expected that when the near-wall ODT is coupled within the TLS formulation, we will be able to capture both near-wall and far-field behavior within a single formulation. Note that the small-scale 1D model used in the TLS approach is actually an extension of the near-wall ODT and therefore, coupling of both these methods is not expected to be a major hurdle.

5 Conclusions

A new TLS approach alternative to LES has been developed based on the decomposition of velocity into resolved and small-scale components. A coupled system of the resolved and small-scale equation that is not based on an eddy-viscosity type of assumption has been derived and implemented to simulate very high-Re wall-bounded turbulent flows as in a channel.

While our approach is intended for turbulent flows governed by Navier-Stokes equations at high Reynolds number, it is first demonstrated here for simpler case of one dimensional randomly forced Burgers equation. The small-scale velocity field can be relatively accurate reconstructed by solving the small-scale equation (33). A solution of this equation is strongly dependent on a forcing term defined by mutual interaction of resolved scales and insensitive to initial conditions imposed on the small-scale velocity. Our numerical model of solving the coupled system of the resolved and small-scale equations showed some predictive potential and can

be easily generalized for three dimensional case of homogeneous turbulence which is a subject of future research.

Preliminary study using a full 3D TLS model of the more complex cases of inhomogeneous turbulent flows governed by the Navier-Stokes equation has been also carried out and some trends and behavior of the TLS model has been discussed in this paper. Results suggest that the baseline TLS model which requires no adjustable parameters has the potential for capturing turbulent flow behavior in high Re channel flows using very coarse grids (e.g., the resolved grid used for TLS is only $32 \times 32 \times 32$ for a $Re_\tau = 595$ (whereas, a $384 \times 257 \times 384$ grid resolution is needed for an equivalent DNS). Further improvements of the TLS model near the wall is planned by using the near-wall ODT model. The application of this combined TLS model to very high Re flows will be reported in the near future.

Acknowledgement

This work is supported by Office of Naval Research.

References

- 1 Moser, R., Kim, J., and Mansour, N., "Direct numerical simulation of turbulent channel flow up to $Re_\tau = 590$," *Journal of Fluid Mechanics*, Vol. 11, 1999, pp. 943-945.
- 2 Baggett, J. S., Jimenez, J., and Kravchenko, A. G., "Resolution Requirements in Large-Eddy Simulations of Shear Flows," *Center For Turbulent Research, Annual Research Briefs*, 1997, pp. 51-66.
- 3 Schmidt, R., Kerstein, A., Wunsch, S., and Nilsen, V., "Near-Wall LES CLOSure Based on One-Dimensional Turbulence Modeling," *Journal of Computational Physics*, 2000, pp. submitted.
- 4 Piomelli, U. and Balaras, E., "Wall Layer Models for Large-Eddy Simulation," *Annual Review of Fluid Mechanics*, Vol. 34, 2002, pp. 349-374.
- 5 Smagorinsky, J., "General Circulation Experiments with the Primitive Equations," *Monthly Weather Review*, Vol. 91, No. 3, 1993, pp. 99-164.
- 6 Schumann, U., "Subgrid Scale Model for Finite Difference Simulations of turbulent Flows in Plane Channels and Annuli," *Journal of Computational Physics*, Vol. 18, 1975, pp. 376-404.
- 7 Germano, M., Piomelli, U., Moin, P., and Cabot, W. H., "A Dynamic Subgrid-Scale Eddy viscosity Model," *Physics of Fluids A*, Vol. 3, No. 11, 1991, pp. 1760-1765.
- 8 Piomelli, U., Cabot, W. H., and Moin, P., "Subgrid-Scale Backscatter in Turbulent and Transitional Flows," *Physics of Fluids A*, Vol. 3, 1991, pp. 1766-1766.

- ⁹ Leith, C., "Stochastic backscatter in a subgrid scale model: plane shear mixing layer," *Physics of Fluids*, 1990, pp. 297–299.
- ¹⁰ Schumann, U., "Stochastic Backscatter of Turbulence Energy and Scalar Variance by Random Subgrid-Scale Fluxes," *Journal of Fluid Mechanics*, Vol. 451, 1995, pp. 293–293.
- ¹¹ Menon, S., Yeung, P.-K., and Kim, W.-W., "Effect of Subgrid Models on the Computed Interscale Energy Transfer in Isotropic Turbulence," *Computers and Fluids*, Vol. 25, No. 2, 1996, pp. 165–180.
- ¹² Domaradzki, J. and Saiki, E., "A subgrid-scale model based on the estimation of unresolved scales of turbulence," *Physics of Fluids*, Vol. 9, 1997, pp. 2148–2164.
- ¹³ Laval, J., Dubrulle, B., and Nazarenko, S., "Nonlocality of interaction of scales in the dynamics of 2D incompressible fluids," *Phys.Rev.Let.*, Vol. 83, 1999, pp. 4061–4064.
- ¹⁴ Laval, J., Dubrulle, B., and Nazarenko, S., "Dynamical modeling of sub-grid scales in 2D turbulence," *Physica D*, Vol. 142, 2000, pp. 231–253.
- ¹⁵ Laval, J., Dubrulle, B., and Nazarenko, S., "Nonlocality and intermittency in three-dimensional turbulence," *Physics of Fluids*, Vol. 13, 2001, pp. 1995–2012.
- ¹⁶ Foias, C., Manley, O., and Temam, R., "Modeling on the interaction of small and large eddies in two-dimensional turbulent flows," *Mathematical Modelling and Numerical Analysis*, Vol. 22, 1988, pp. 93–114.
- ¹⁷ Foias, C., Manley, O., and Temam, R., "Approximate inertial manifolds and effective viscosity in turbulent flows," *Physics of Fluids*, 1990, pp. 898–911.
- ¹⁸ Dubois, T., Jauberteau, F., and Temam, R., *Dynamic multilevel methods and the numerical simulation of turbulence*, Cambridge University Press, 1999.
- ¹⁹ Hughes, T., Feijo, G., L.Mazzei, L., and Quincy, J.-B., "The variational multiscale method- a paradigm for computational mechanics," *Computer Methods in Applied Mechanics and Engineering*, Vol. 166, 1998, pp. 3–24.
- ²⁰ Hughes, T., Mazzei, L., and Jansen, K., "The Large Eddy Simulation and variational multiscale method," *Comput. Vis.Sci.*, Vol. 3, 2000, pp. 47–59.
- ²¹ Hughes, T., Mazzei, L., and Oberai, A., "The multiscale formulation of Large-eddy simulation: Decay of homogeneous isotropic turbulence," *The Physics of Fluids*, Vol. 13, 2001, pp. 505–512.
- ²² Scotti, A. and Meneveau, C., "A fractal model for large eddy simulation of turbulent flow," *Physica D*, Vol. 127, 1999, pp. 198–232.
- ²³ Hylin, E. and McDonough, J., "Chaotic small-scale velocity fields as prospective models for unresolved turbulence in an additive decomposition of the Navier-Stokes equation," *International Journal of Fluid Mechanics Research*, Vol. 26, 1999, pp. 539–567.
- ²⁴ Kerstein, A., "One-dimensional turbulence: model formulation and application to homogeneous turbulence, shear flows and buoyant stratified flows," *Journal of Fluid Mechanics*, Vol. 392, 1999, pp. 277–334.
- ²⁵ Kerstein, A., Ashurst, W., Wunsch, S., and Nilsen, V., "One-dimensional turbulence: vector formulation and application to free shear flows," *Journal of Fluid Mechanics*, Vol. 447, 2001, pp. 85–109.
- ²⁶ van Kan, J., "A second-order accurate pressure-correction scheme for viscous incompressible flow," *SIAM Journal of on Scientific and Statistical Computing*, Vol. 7, No. 3, 1986, pp. 870–891.
- ²⁷ Majda, A. and Timofeev, I., "Remarkable statistical behavior for truncated Burgers-Hopf dynamics," *Proceedings of the National Academy of Sciences of the USA*, Vol. 97, 2000, pp. 12413–12417.
- ²⁸ Williamson, J. H., "Low storage Runge-Kutta schemes," *Journal of Computational Physics*, Vol. 35, No. 1, 1980, pp. 48–56.